Automotive fuel cell stack and system efficiency and fuel consumption based on vehicle testing on a chassis dynamometer at minus 18°C to positive 35°C temperatures

Henning Lohse-Busch, Kevin Stutenberg, Michael Duoba, Xinyu Liu, Amgad Elgowainy, Michael Wang, Thomas Wallner, Argonne National Laboratories
Brad Richard, Martha Christenson, Transport Canada

Abstract

This paper presents an in-depth laboratory technology assessment of a 2016 Toyota Mirai Fuel Cell (FC) vehicle based on chassis dynamometer testing. The 114.6 kW FC stack has a high dynamic response which makes this powertrain a FC-dominant hybrid electric vehicle. The measured peak efficiency is 66.0% FC stack and 63.7% FC system with an idle hydrogen flow rate of 4.39 g/hr. The high FC system efficiencies at low loads match typical vehicle power spectrums, thus resulting in a high average vehicle efficiency of 62% compared to 45% and 23% for a hybrid electric vehicle and a conventional vehicle respectively. An energy breakdown accounts for the FC stack losses, FC system losses, air compressor loads, and heater loads for different drive cycles and different thermal conditions. The cold-start North American city drive cycle (UDDS) energy consumption are 758, 581, 226, 321 Wh/km at ambient conditions of -18°C, -7°C, 25°C and 35°C with 850 W/m² of solar loading. The FC system shutdown and start up process at temperatures below the freezing point contribute to the increased hydrogen consumption. The raw test data files are available for download, thus providing a public reference data production on a modern automotive FC system to the research community.

1. Introduction

1.1. Lack of public automotive fuel cell system data

Although several companies have researched hydrogen powered fuel cell (FC) vehicles since the 1990s (Lynn K. Mytelka, 2008), and despite the presence of six production FC vehicles in the North American market, the research community is lacking public, independent, laboratory-grade data on modern production FC vehicles. The U.S. Department of Energy's (DOE) Fuel Cell Technologies Office identified the "lack of fuel cell electric vehicle [...] performance and durability data" as a technical barrier in its multi-year research, development, and demonstration plan (Fuel Cell Technologies Office, 2012, updated 2016). The 2015 value of 60% peak energy efficiency of an 80-kW integrated transportation FC power system (Fuel Cell Technologies Office, 2015) was based on a paper (Woosuk Sung, 2010), which references 65% stack and 62% system efficiency at 60 mile per hour (mph).

The National Renewable Energy Laboratory performed an on-road evaluation of several different FC vehicles and showed a peak mean FC stack efficiency of 67% and a reported peak FC system efficiency of 58% through analysis of the anonymized and normalized FC data (Kurtz, 2016). Other publications (Kumar, 2018) (Salman, 2017) (Chubbock, 2016) discuss automotive FC efficiencies, but none provide laboratory tested stack and system efficiency curves of modern automotive production FC systems. Finally, much research (Ahmadi P, 2017), (Ahmadi P T. S., 2019), (Elgowainy A, 2018) relies on high fidelity simulation models, which were validated using overall fuel economy data or proprietary FC system data.

1.2. Fuel economy overview of production fuel cell vehicles

The U.S. Environmental Protection Agency (EPA) provides official fuel economy test results based on standard drive cycles and testing conditions. Table 1 summarizes the fuel economy results for all FC vehicles posted to EPA's Test Car Data list (U.S. Environmental Protection Agency, 2019). The first part of the table summarizes the vehicle characteristics, such as equivalent test weight and the road load force coefficients, used for the chassis dynamometer testing (Lohse-Busch, 2013). Next, the unadjusted hydrogen fuel consumption results for the city drive cycle (FTP: Federal Test Procedure) and the highway drive cycle (HWFET: Highway Fuel Economy Test) tested at an ambient temperature of 25°C (72°F) are shown. Finally, the calculated vehicle efficiencies, as defined in section 3.1, are provided.

Table 1: Summary of EPA test car list data on fuel cell vehicles and their calculated vehicle efficiency

	Ve	hicle Test	: Characte	ristics	Fu	usted el nption	Calcu Veh Effici		
Model (model year)	Equivalent Test Weight [kg]	Target A Term [N]	Target B Term [N/(m/s)]	Target C Term [N/(m/s)²]	FTP City [Wh/km]	FET Highway [Wh/km]	FTP Vehicle Efficiency [%]	FET Vehicle Efficiency [%]	
Honda FCX Clarity (2011–2014)	1758	165.4	1.032	0.4236	254	248	54%	51%	
Mercedes-Benz F-Cell (2011–2012)	1814	23.0	0.000	0.5039	284	275	40%	35%	
Hyundai Tucson Fuel Cell (2015–2017)	2041	136.7	4.364	0.4721	311	294	51%	51%	
Toyota Mirai (2016–2019)	1928	143.8	1.990	0.4072	220	220	65%	58%	
Honda Clarity Fuel Cell (2018–2019)	2041	134.8	1.032	0.4367	218	220	67%	57%	
Hyundai Nexo (2019)	2041	188.8	-0.182	0.6344	245	269	66%	58%	
Hyundai Nexo Blue (2019)	1928	163.2	-0.101	0.6201	222	251	68%	59%	

Between 2011 and 2019, the vehicle efficiencies increase from around 50% to 65% or higher for the city drive cycle. The Toyota Mirai, Honda Clarity, and Hyundai Nexo have very similar high levels of vehicle efficiency. The 2016 Toyota Mirai, which is the car tested in this technology assessment, is one of the highest-efficiency FC vehicles and thus is representative of modern FC technology.

1.3. Public and independent 10-Hz data on a modern fuel cell system

Argonne, in a collaboration with Transport Canada (Argonne National Laboratory, 2018), performed a comprehensive laboratory-based technology assessment of a production FC vehicle with the goal of generating public and independent data for the FC research community. The key findings are the measured automotive FC stack and system performance and efficiency curves. These efficiency curves and the data are intended to help refine and validate modeling and simulation work, to inform the research target setting process, and to highlight potential challenges that necessitate further research.

2. Materials and methods

2.1. Details on the production fuel cell vehicle tested

Transport Canada provided a 2016 Toyota Mirai for this testing. Table 2 provides a summary of relevant vehicle information.

Table 2: Test setup parameters and powertrain specifications of the 2016 Toyota Mirai

Vehicle Architecture	FC Series Hybrid Vehicle						
Equivalent Test Weight (1)	1928 kg (4250 lb)						
Road Load (1)	A = 143.8 N	(32.325 lbf)					
	B = 1.990 N/(m/s)	(0.20003 lbf/mph)					
	$C = 0.4072 \text{ N/(m/s)}^2$ (0.018292 lbf/mph ²						
FC System (2)	Solid Polymer Electrol	yte Fuel Cell					
	370 cells in stack						
	114 kW, 3.1 kW/L, 2.0 kW/kg						
Battery (2)	Nickel-metal Hydride,	1.6 kWh, 245 V DC					

^{(1) (}U.S. Environmental Protection Agency, 2019), (2) (Toyota, 2017)

2.2. Vehicle research test facility

Argonne's automotive test facility was built for powertrain research and technology benchmarking. The chassis dynamometer is housed in a thermal chamber, which allows testing under a range of real-world conditions. The test conditions are based on the EPA 5-cycle label fuel economy procedures, which include ambient temperatures of -7°C (20°F), 25°C (72°F), and 35°C (95°F), with 850 W/m² of radiant solar emulation. Additional testing occurred at -18°C (0°F). The research staff has developed and refined deep expertise in the instrumentation of advanced technology powertrain components. At the center of the vehicle instrumentation is a custom integrated data acquisition system that merges and time-aligns data streams from many different selectable sources.

2.3. In-depth instrumentation overview

The instrumentation focus is on measuring the power flows between the major powertrain components, as shown in Figure 1. A Hioki™ high-precision power analyzer (PW3390-10) was used to measure the electrical power flows with an accuracy of +/- 0.1%. The hydrogen mass flow was measured with two Micro Motion™ Coriolis mass flow meters (low flow range CMF010M and high flow range CMF025M) integrated into the test cell with a gas flow accuracy of +/- 0.25%. Many relevant digital messages from the Controller Area Networks (CAN) were decoded. Over 400 significant signals were recorded at 10 Hz for the more than 100 tests. For more detail on Argonne's approach to chassis dynamometer testing and instrumentation, refer to the Chassis Dynamometer Testing Reference Document (Lohse-Busch, 2013).

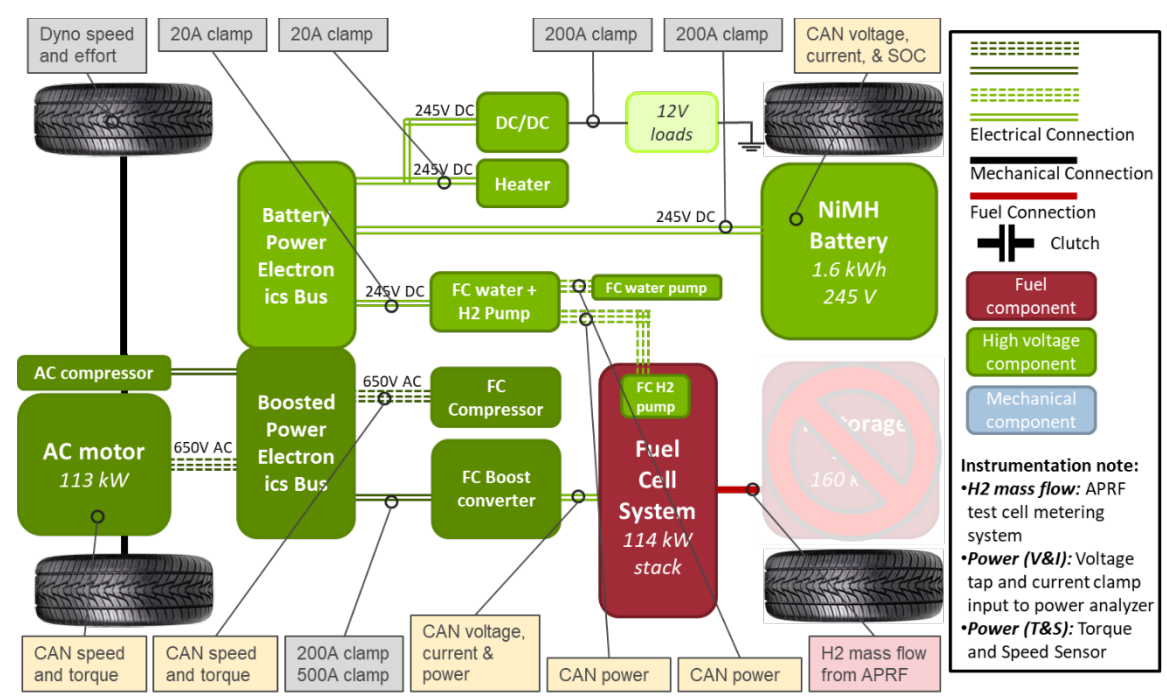


Figure 1: Power flow instrumentation summary.

2.4. Vehicle setup on the chassis dynamometer

The EPA vehicle equivalent test weight and road load coefficients for the Toyota Mirai, shown in Table 2, are used for this testing. The vehicle losses, which are vehicle losses present during chassis dynamometer testing only, are derived on the chassis dynamometer and are based on SAE J1263™, "Road Load Measurement and Dynamometer Simulation Using Coastdown Techniques" (Society of Automotive Engineers, 2010). To minimize the test-to-test variability inherent in vehicle re-mounting, the vehicle was left on the chassis dynamometer for the duration of the testing. This setup yields to a test to test repeatability of less than 2% on fuel consumption. The test cell cooling fan was run dynamically to match the air flow speed to the vehicle speed, and the vehicle hood was closed for all testing, regardless of ambient temperature, to emulate real-world conditions. The SAE J2951™ "Drive Quality Evaluation for Chassis Dynamometer Testing" (Society of Automotive Engineers, 2014) metrics are calculated at the end of each test and are published with the data.

2.5. Hydrogen fuel specifications

The hydrogen used for the testing was "ultra high purity 5.0 grade hydrogen" procured through Airgas. The energy content of hydrogen is based on the Lower Heating Value (LHV) of 119.96 MJ/kg (National Institute of Standards and Technology, 2018).

3. Theory and calculations

3.1. Fuel cell stack and fuel cell system efficiency calculations

Efficiency is defined as the electric output energy divided by the hydrogen input energy of the system. Figure 2, which focuses on the FC system shown in the powertrain schematic of Figure 1, defines the FC stack boundaries and the FC system boundaries considered in this work.

Equation 1 and Equation 2 define the FC stack and FC system efficiencies respectively. Note that these equations maybe applied over a full drive cycle or over shorter time segments.

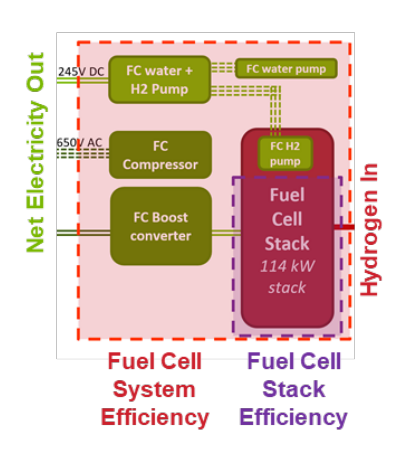


Figure 2: FC stack and system boundary definition

Equation 1: FC stack efficiency calculation, where V stands for Voltage and I stands for Current

$$Efficiency_{FCstack} = \frac{\int_{t_{initial}}^{t_{final}} V_{FCstack}(t) \times I(t) dt}{\int_{t_{initial}}^{t_{final}} MassFlow_{Hydrogen}(t) \times LHV dt}$$

Equation 2: FC system efficiency calculation, where V stands for Voltage and I stands for Current

$$Efficiency_{FCsystem} = \frac{\int_{t_{initial}}^{t_{final}} \left[V_{BoostConv}(t) \times I_{BoostConv}(t) - Power_{FCcomp}(t) - V_{HVbattery}(t) \times I_{Water\&H_2Pump}(t) \right] dt}{\int_{t_{initial}}^{t_{final}} MassFlow_{Hydrogen}(t) \times LHV dt}$$

3.2. Vehicle efficiency calculation

The vehicle efficiency is calculated by dividing the positive cycle energy by the fuel energy as shown in Equation 3. The positive cycle energy is defined in SAE J2951™, "Drive Quality Evaluation for Chassis Dynamometer Testing" (Society of Automotive Engineers, 2014). The standard clearly prescribes the data processing and calculation steps to generate the positive cycle energy parameter, among many other useful testing parameters. This standard was developed from the conventional-vehicle standpoint. Note that within this work the vehicle efficiency is only calculated for full drive cycles.

Equation 3: Vehicle efficiency calculation

$$Efficiency_{Vehicle} = \frac{SAE\,J2951\,Posible\,Cycle\,Energy}{\int_{t_{initial}}^{t_{final}} MassFlow_{Hydrogen}(t) \times LHV_{Hydrogen}\,dt}$$

3.3. Standard certification drive cycles

Drive cycles are specific speed profiles defined as a function of time. Three major certification cycles were used in this assessment:

• **UDDS:** The Urban Dynamometer Driving Schedule is a city drive profile with mild accelerations. The Federal Test Procedure (FTP) for city fuel economy is composed of a cold-start UDDS,

followed by a hot-start UDDS after a 10 minute key-off break. A "cold start" test means that the vehicle, and therefore the powertrain, was soaked at the target ambient temperature for over 12 hours before the start of the test.

- Highway: The highway cycle is the drive cycle of the Highway Fuel Economy Test (HWFET)
- US06: The US06 is a cycle designed with very aggressive accelerations and high-speed sections.

The graph in Figure 3 shows the sequence of drive cycles executed for this testing. The fuel consumption results are reported for the test phases highlighted by the green boxes.

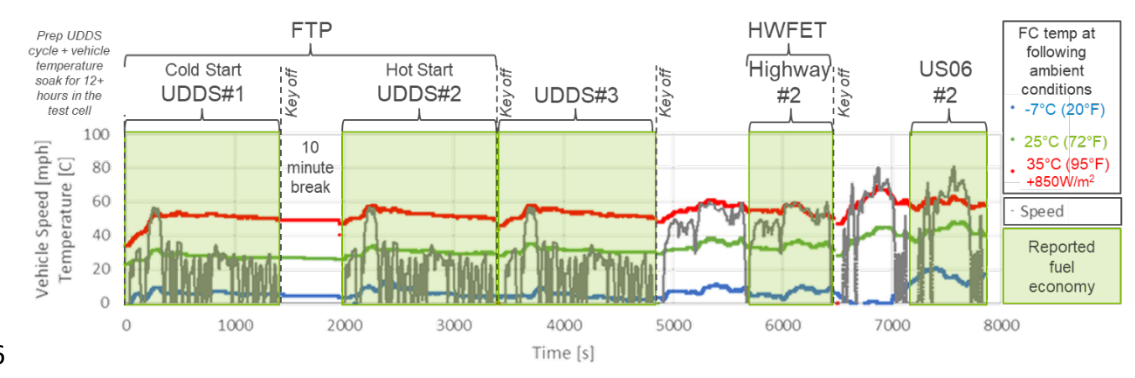


Figure 3: Standard drive cycle test sequence.

4. Results and discussion

4.1. Fuel cell system and hybrid system operation

This powertrain is a FC-dominant hybrid. Like the internal combustion engine in a mild hybrid electric vehicle, the FC stack provides the majority of the traction power, and typically does not operate while the vehicle is stopped, and has the ability to turn off or idle to enable the car to operate momentarily as an electric vehicle. The open-circuit voltage (OCV) slowly decreases as the FC system idles. Figure 4 illustrates these different powertrain operating modes on the New European Driving Cycle. The dyno power, or wheel power, is the power required to drive the vehicle on the drive cycle. The dyno power is the sum of the FC stack power, the high voltage battery power and the auxiliary power losses.

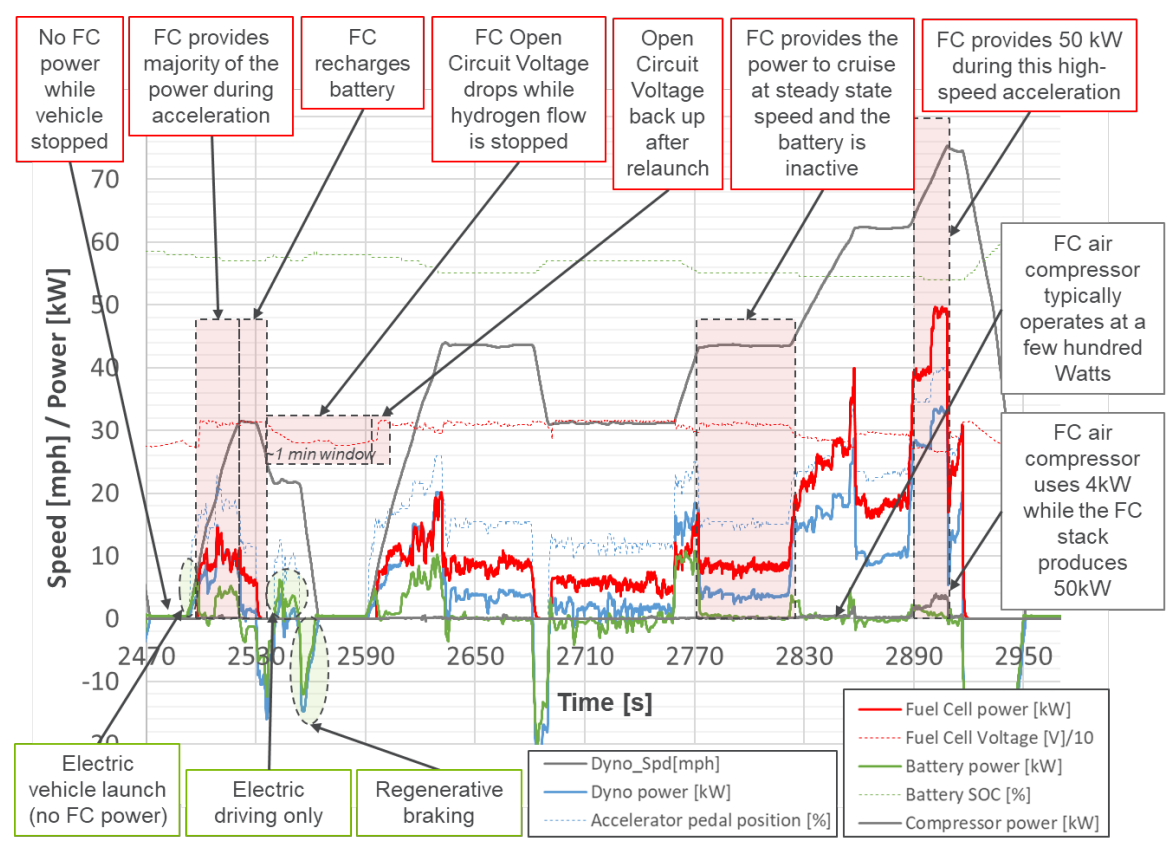


Figure 4: Powertrain and fuel cell system operation in different drive modes on a linear segment drive cycle.

4.2. Fuel cell stack and system efficiency curve

The vehicle was tested at different steady-state speeds and steady-state load points to establish a FC stack and system efficiency map. The FC stack, FC system, and boost converter efficiencies, shown in Figure 5, were derived from the 10-Hz data generated by the instrumentation and using Equation 1 and Equation 2.

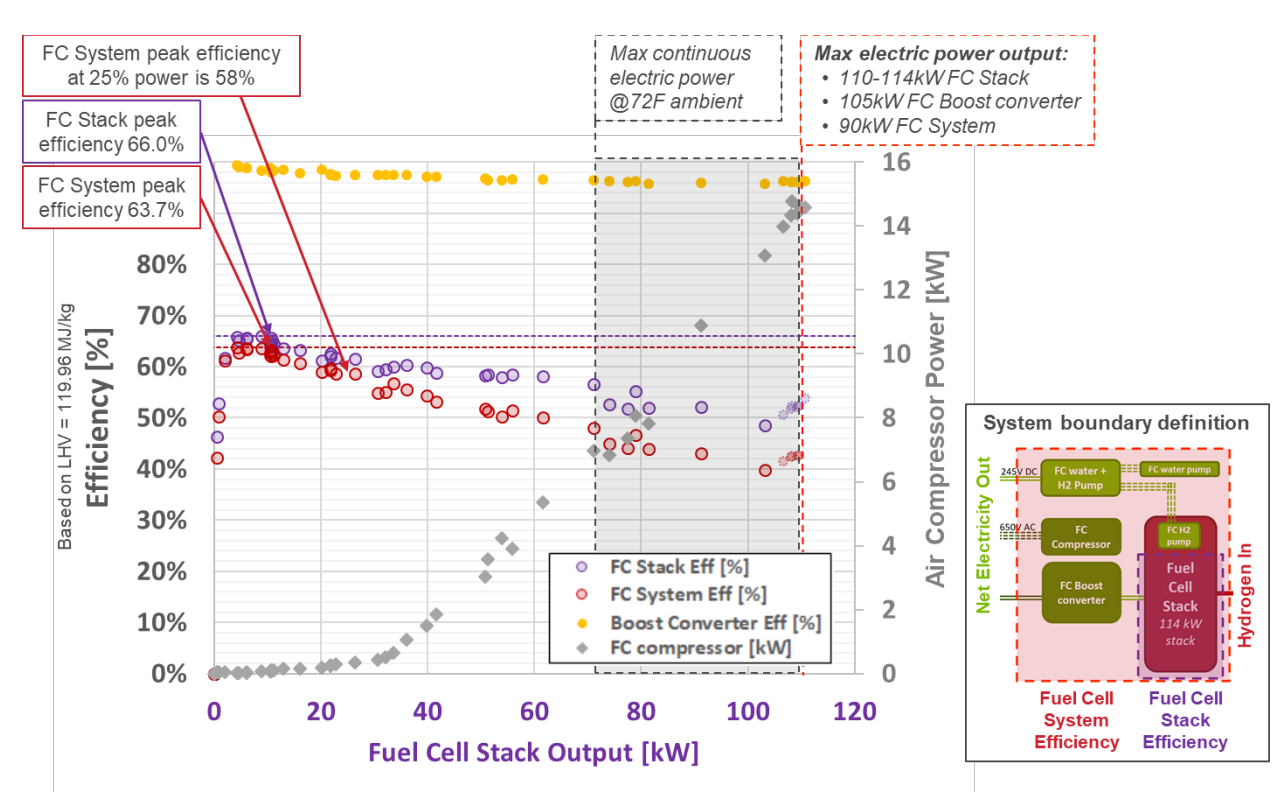


Figure 5: Fuel cell stack and fuel cell system efficiency as a function of electric power output of the stack

The measured FC stack peak efficiency is 66.0%. The measured FC system peak efficiency is 63.7%. The FC system efficiency at 25% of maximum power is 58%. The low air-compressor power consumption of a 100W to 400W at low stack power (<30 kW) results in high system efficiencies. Most of the certification drive cycles, as well as typical drive conditions, are characterized by such low power demands; therefore, the FC system typically operates in its most efficient range. The air management system and anode flow channels were specifically redesigned to minimize the auxiliary power losses to the air compressor in this generation of Toyota FC system (Hasegawa, 2016). The maximum power output of the FC stack was measured at around 110 to 114 kW, depending on the thermal conditions. At these high-power levels, the air compressor consumes up to 15 kW, penalizing the FC system efficiency.

4.3. The fuel cell system efficiency curve shape is advantageous for most driving

Figure 6 shows the power spectrum the vehicle needs to complete each drive cycle. Note that 90% of the time, the power needed to complete the cycle is less than 12 kW and 20 kW for the UDDS and Highway cycles, respectively. The low power demand on the FC system keeps that average FC system efficiency above 61% on the UDDS and Highway cycles. In contrast, the US06 cycle requires higher power levels from the FC system, for which the air-compressor loads become more significant. Therefore, the average FC system efficiency is below 50% while the stack efficiency is still above 61% on the US06 cycle.

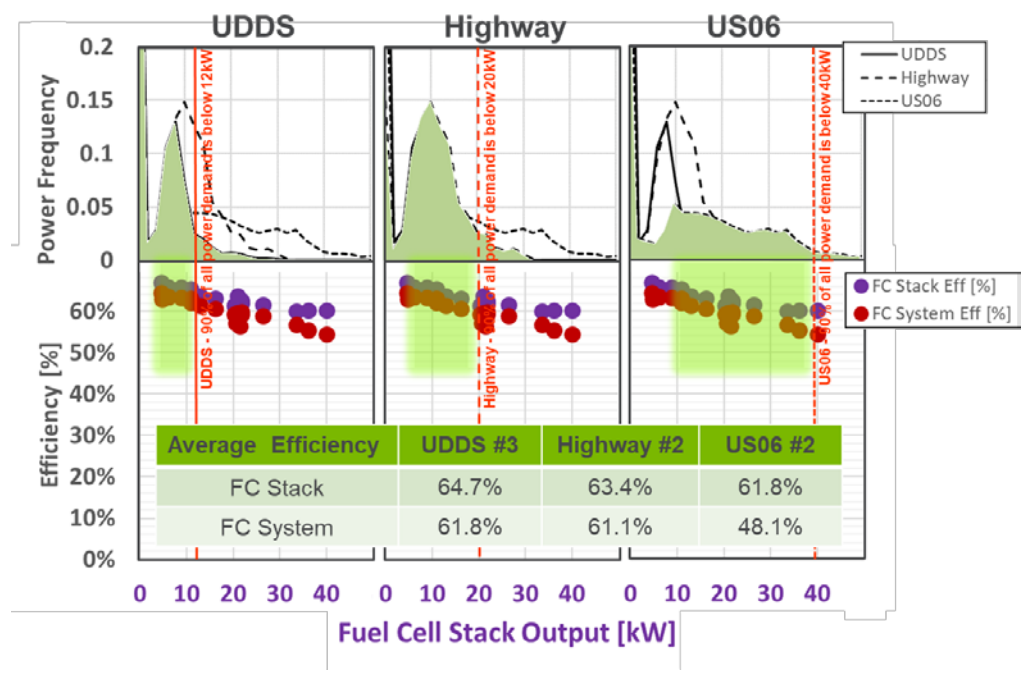


Figure 6: Power spectrum of the standard certification drive cycles

The high FC system efficiency at low loads should translate to low fuel consumption under real-world conditions, as the mean power loads for the typical drives are low. In contrast, the brake thermal efficiency of an internal combustion engine increases with increasing load (Heywood, 1988).

4.4. Determining the fuel cell system idle fuel flow rate.

As noted in Figure 4, the FC system turns "off" when FC power is not needed. This FC idle condition produces zero electric power output. To investigate this idle operation, a special 1-hour test was performed. After 505 seconds of driving, the vehicle was put in park and left "on." The FC system produced no electric power for 1400 seconds. The data show that the FC stack was starved for hydrogen to maintain an open-circuit stack voltage around 74 V (a typical OCV is 315 V). Periodically (~ every 40 seconds), a small amount of hydrogen was released in the system and air was pushed into the stack to maintain enough reactants in the stack. Over the 1400 seconds of idle, 1.71 g of hydrogen was consumed, resulting in an idle fuel flow rate of 4.39 g/hr. The low idle fuel flow rate enables the FC system to have enough reactants in the channels to provide immediate power when needed. After the 1400 seconds of idle, the state of charge of the high-voltage battery pack had dropped low enough that the FC system produced power to recharge the battery pack. Note that if the FC stack does not produce any power, the hydrogen flow is zero for the first 40 seconds to a minute.

4.5. Peak fuel cell stack power

At 25°C (72°F) on a simulated 25% grade, the FC stack produced 112 kW for 30 seconds and the continuous FC stack power settled at 73 kW with a terminal vehicle and fan speed of 43 kilometer per hour (kph) (27 mph). At 35°C (95°F), with 850 W/m² of solar load emulation on a simulated 25% grade with the climate control system set to a 25°C (72°F) cabin temperature, the FC stack settled at 50 kW with a terminal vehicle and fan speed of 24 kph (15 mph). At 35°C (95°F), with 850 W/m² of solar load emulation on a simulated 6% grade with the climate control system set to a 25°C (72°F) cabin temperature and the vehicle loaded to a gross vehicle weight of 2182 kg (4810 lbs), the vehicle

maintained 100 kph (62 mph) for the 30 minutes of the test. In this realistic worst-case scenario, the FC stack power output settled at 63 kW while the test cell cooling fan was providing air at 100 kph (62 mph). The maximum continuous power will depend on the thermal and cooling conditions.

Finally, four back-to-back maximum accelerations from a rolling start to 129 kph (80 mph) were tested at 25°C (72°F). As is the case with most mild hybrid vehicles, the high voltage battery pack did not provide any assistance on the last acceleration, as the battery depleted over the first few acceleration runs. The peak FC power increased from 100 kW on the first acceleration run to 114.6 kW on the last acceleration run.

The continuous maximum power is highly dependent on the cooling conditions, such as ambient temperature and relative wind speed. All the testing was performed with a variable-speed fan that matched the vehicle speed. In realistic high-power scenarios, the FC system provided all the requested power reliably and repeatably to the powertrain.

4.6. Vehicle efficiency comparison between different vehicle types

Table 3 compares a fuel cell, a battery electric, a hybrid electric, and a conventional powertrain from a vehicle efficiency standpoint as defined in Section 3.1. Note that the vehicle efficiency is calculated using only the positive power required to complete the drive cycle, to be compatible with conventional vehicles, which convert the braking power into heat. This calculation is more complex for electrified vehicles, which during braking recover the kinetic and potential energy by storing it in a high voltage battery pack. The bi-directional power flow in electrified powertrains can result in calculating vehicle efficiencies at over 100% when using only the positive cycle energy. Table 3 is based on data of vehicles tested at Argonne in the same test cell. The full fuel and energy consumption results, along with vehicle details, are provided in Appendix A. The Toyota Prius Prime in charge-depleting mode can drive all three drive cycles in full electric mode, and thus is representative of a battery electric vehicle. Once its battery is depleted, the Toyota Prius Prime operates in charge-sustaining mode, and thus is representative of a hybrid electric vehicle. The Mazda 3 is a conventional vehicle comparable to the Toyota Mirai as a small to mid-size sedan also tested in the same laboratory and conditions.

Table 3: Vehicle efficiency* comparison across powertrain architectures

Powertrain Type	Fuel Cell Vehicle			Battery Electric Vehicle			Hybrid Electric Vehicle			Conventional Vehicle		
Representative Model	2016 Toyota Mirai			2016 Toyota Mirai 2017 Toyota Prius 2017 Toyota Prius Prime in charge- depleting mode 2017 Toyota Prius Prime in charge- sustaining mode				2014 Mazda 3 (2.5L i- ELOOP)				
Test Temperature	- 7°C (20°F)	25°C (72°F)	35°C (95°F)	- 7°C (20°F)	25°C (72°F)	35°C (95°F)	- 7°C (20°F)	25°C (72°F)	35°C (95°F)	- 7°C (20°F)	25°C (72°F)	35°C (95°F)
UDDS#1	24.6	62.8	24.6	52.4	109.8	81.8	32.4	48.6	33.6	14.1	18.7	17.2
UDDS#2	40.8	65.7	40.8	56.8	112.5	91.4	30.8	48.0	36.2	19.1	20.8	18.3
UDDS#3	54.9	67.7	54.9		113.4	91.3		49.9	40.0	19.4	20.8	17.8
Highway#2	55.7	57.6	55.7	54.0	82.2	77.0	33.0	39.1	35.8	26.5	28.7	28.1
US06#2	52.5	57.1	52.5	72.8	91.2	87.0	39.3	43.0	39.2	27.5	28.4	28.2
Average	45.7	62.2	45.7	59.0	101.8	85.7	33.9	45.7	37.0	21.3	23.5	21.9
	*Vehic	*Vehicle efficiency in [%] based on positive cycle energy as defined by SAE J2951 ™										

The FC vehicle has a significant vehicle efficiency advantage (62.2% average at 25°C) over the hybrid electric vehicle (45.7% average at 25°C) and conventional vehicle (23.5% average at 25°C) due to the higher conversion efficiency of the FC system. A FC vehicle, which is a series hybrid electric vehicle, is an electric vehicle with a smaller battery pack and a FC system that provides most of the power. Therefore, the FC vehicle efficiency is based on the electric vehicle efficiency paired with the FC system efficiency. Thus, the FC vehicle has a lower vehicle efficiency compared to a battery electric vehicle. Finally, it is observed that the FC vehicle efficiency is less sensitive to temperature conditions compared to a battery electric vehicle.

A comparison of well to wheels (WTW) energy use and emissions shows that the FC vehicle, even fueled by hydrogen from a fossil-based production pathway (via steam methane reforming of natural gas), reduces the WTW fossil energy use by 4-31% and the WTW GHG emission by 14-44%, compared to gasoline conventional vehicle (Liu X., 2019).

4.7. Energy analysis on standard drive cycles across different temperatures

The hydrogen energy consumption and a loss breakdown are shown in Figure 7. The energy consumption at 25°C (72°F) for the UDDS and Highway drive cycles is similar. On these low-load drive cycles, the losses attributed to the FC air compressor and boost converter are almost insignificant. On the higher-power US06 cycle, the boost converter and air compressor losses become significant, reducing the FC system efficiency as shown in Figure 5.

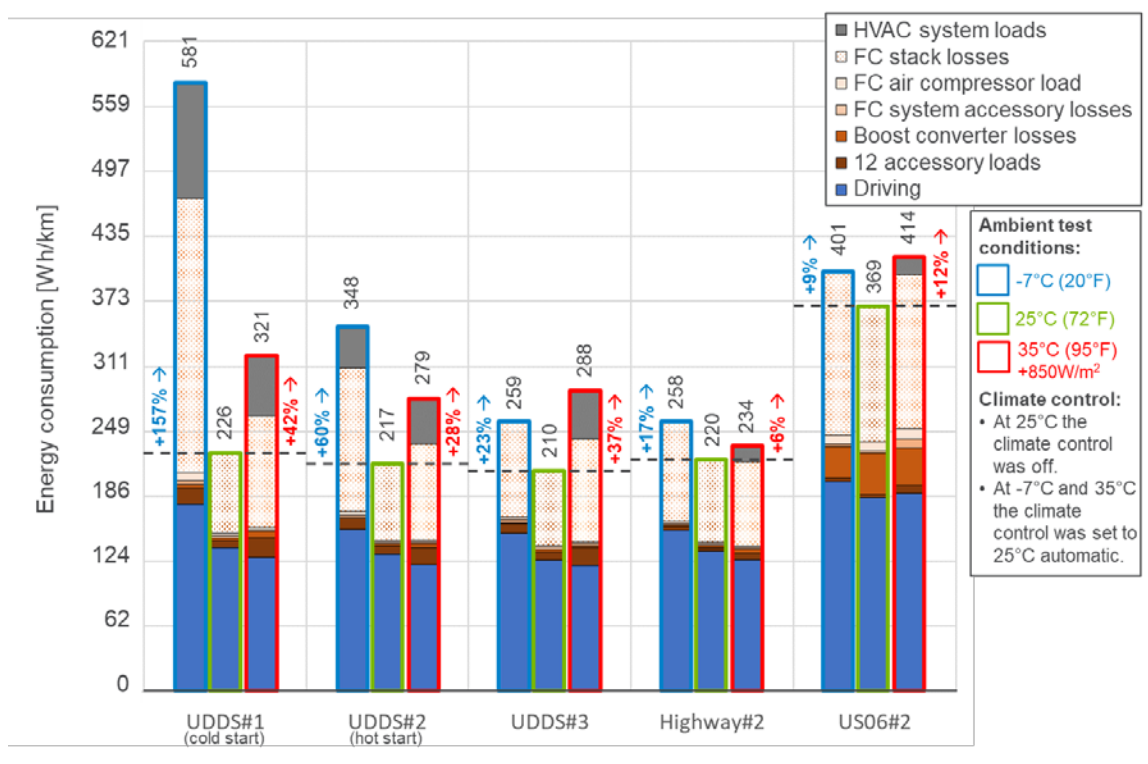


Figure 7: Hydrogen energy consumption and energy breakdown for different drive cycles across different temperatures.

Results for the different ambient conditions tested are also presented in Figure 7. The cold-start UDDS energy consumption at -7°C (20°F) is 150% higher than at 25°C (72°F) because of the electric heating of

the FC system and the cabin as well as the use of additional hydrogen to recondition the dried-out proton exchange membranes. It is noteworthy that the FC system generates enough heat to maintain a cabin temperature of 25°C (72°F) on the third UDDS cycle in a -7°C (20°F) environment. Battery electric vehicles require the use of the electric heater to maintain cabin temperatures in freezing environments even after extensive driving. The energy consumption increase at 35°C (95°F) ambient temperature with the 850 W/m² solar energy emulation is driven by the power demand of the high-voltage refrigerant compressor for the climate control system.

4.8. Fuel cell system startup and shutdown at 25°C (72°F) and -7°C (20°F)

It is critical for a FC system to control the humidity of the proton exchange membranes within the stack in order to generate a reliable and efficient power output. On shutdown, the system has to evacuate the water from the stack to avoid freezing and damages as temperatures drop below 0°C. Figure 8 and Figure 9 detail the system behavior on startup during a cold-start test, as well as during the shutdown of the system at the end of the test. At 25°C (72°F), the FC system does not produce any power until the wheels spin, at which point the stack voltage jumps to stable operating voltages. When the driver turns the vehicle off at the end of the test, the hydrogen is purged out of the stack and air is blown through the stack for about 20 seconds. At -7°C (20°F), the shutdown is prolonged, and hydrogen and air are both used to purge the stack for 90 seconds to dry out the proton exchange membranes. On startup at -7°C (20°F), the FC system uses excess hydrogen and produces low levels of power immediately to generate water from the electro-chemical conversion reaction in order to create optimal humidity conditions for the proton exchange membrane.

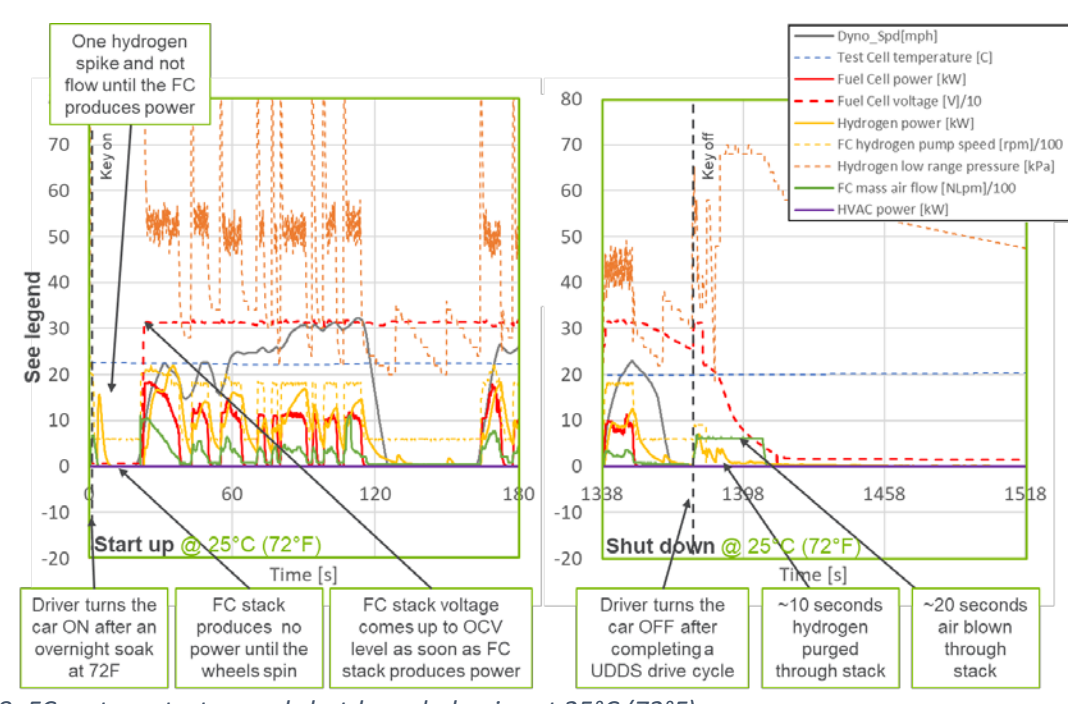


Figure 8: FC system startup and shutdown behavior at 25°C (72°F).

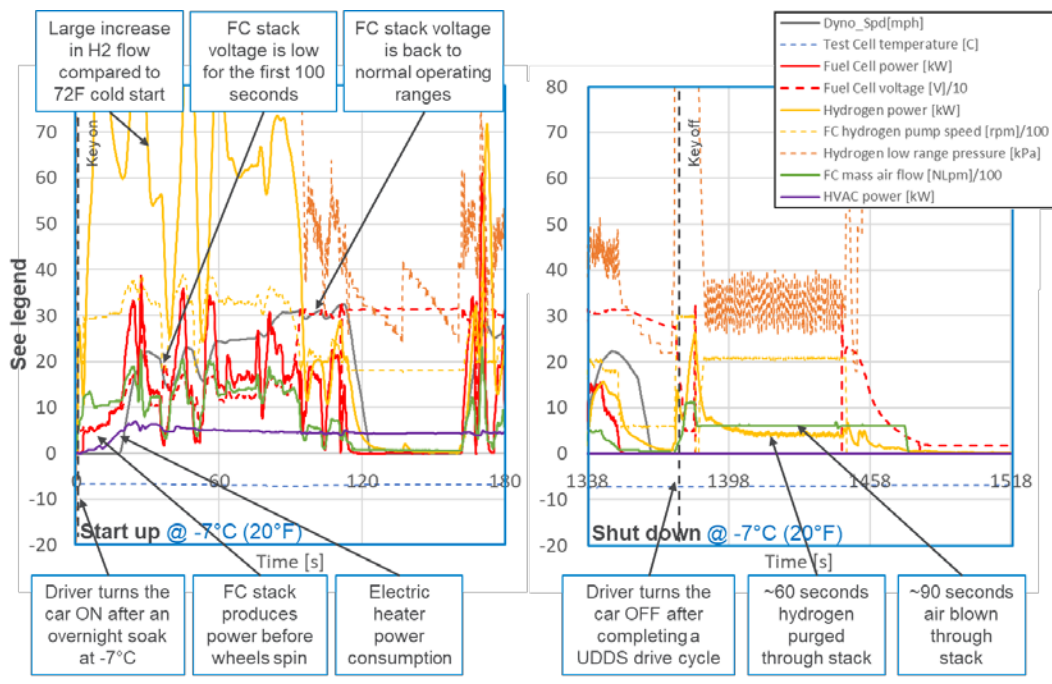


Figure 9: FC system startup and shutdown behavior at -7°C (20°F)

It should be noted that when the ambient air transitions from 25°C to -7°C and the vehicle is turned off, the FC system will wake up to purge the stack and activate the drain valve.

4.9. Cold start after a thermal soak at -18°C (0°F)

The vehicle was temperature soaked over a full weekend at -18°C (0°F). At the start of the test, the electric heater warms up the FC system and extra hydrogen is used to recondition the dry proton exchange membranes. On the cold-start UDDS cycle, the driving starts 20 seconds after the vehicle is turned on. The standard OCV is achieved after 150 seconds of operation. The FC stack power output is limited during these first 150 seconds of the drive cycle, but the battery pack provides extra power to the vehicle to meet the acceleration demands. The fuel consumption on the -18°C (0°F) cold-start UDDS cycle is 135% higher than at 25°C (72°F), as shown in Table 4.

Table 4: Hydrogen fuel consumption* for different drive cycles and temperatures from -18°C (0°F) to 35°C (95°F) with 850 W/ m^2 of solar load

	Ambient Thermal Conditions									
	-18°C (0°F)	-7°C (20°F)	25°C (72°F)	35°C (95°F) + 850 W/m ²						
UDDS#1 Cold start	758	581	226	321						
UDDS#2 Hot start	508	348	217	279						
UDDS#3	477	259	210	288						
Highway#2		258	220	234						
US06#2		401	369	414						

^{*}Hydrogen consumption in [Wh/km]

5. Conclusions

A comprehensive technology assessment of a 2016 Toyota Mirai FC vehicle using a chassis dynamometer with in-depth instrumentation was performed in a controlled laboratory environment. The FC stack has a high dynamic response, which enables this powertrain to be a FC-dominant hybrid electric vehicle. The measured peak efficiency is 66.0% and 63.7% for the stack and FC system, respectively. The maximum stack power output was measured around 110 to 114.6 kW. The overall average FC system efficiency on the UDDS drive cycle (mild city driving) is 61.8%, as compared to 48.1% on the US06 drive cycle (aggressive high-speed driving). The FC system efficiency at high load suffers from the air-compressor load, which can be as high as 15 kW. The energy consumption on the cold-start UDDS cycle at -7°C (20°F) is 157% times higher than at 25°C (72°F) because of the electric heating of the FC system and the cabin as well as the hydrogen used to recondition the dried-out proton exchange membranes. At -18°C (0°F), the FC stack power is limited during the first 150 seconds, but the battery pack provides the extra power to meet the acceleration demands. The FC system has an idle fuel flow rate of 4.39 g/hr while producing zero power output. The low idle fuel flow rate enables the FC system to have enough reactants in the channels to provide immediate power when needed.

Importantly, all the 10-Hz test data are available for download to the public at www.anl.gov/d3. Thus, much-needed public reference data on a modern automotive FC system are provided for the research community.

Acknowledgment

The author extends his deep gratitude to Transport Canada's Innovation Centre, which is a Canadian federal government department responsible for transportation R&D. Transport Canada provided the vehicle and engaged in a successful and open exchange of knowledge and ideas. The author is also indebted to the outstanding and talented staff at Argonne's vehicle test facility for their expert knowledge and their dedication to the project.

Funding

This research was supported by the Fuel Cell Technologies Office of the U.S. Department of Energy's Office of Energy Efficiency and Renewable Energy under Contract No. DE-AC02-06CH11357. The authors thank Jason Marcinkoski and Sunita Satyapal from DOE's Fuel Cell Technologies Office for their guidance and support. The views and opinions of the authors expressed herein do not necessarily state or reflect those of the United States Government or any agency thereof. Neither the United States Government nor any agency thereof, nor any of their employees, makes any warranty, expressed or implied, or assumes any legal liability or responsibility for the accuracy, completeness, or usefulness of any information, apparatus, product, or process disclosed, or represents that its use would not infringe privately owned rights.

References

Ahmadi P, K. E. (2017). Realistic simulation of fuel economy and life cycle metrics for hydrogen fuel cell vehicles. *International Journal of Energy Resources*, 41:714–27.

- Ahmadi P, T. S. (2019). The effects of driving patterns and PEM fuel cell degradation on the lifecycle assessment of hydrogen fuel cell vehicles. *International Journal of Hydrogen Energy*, doi:10.1016/J.IJHYDENE.2019.01.165.
- Argonne National Laboratory. (2018, May 10). *Analyzing with impact*. Retrieved from Energy Systems Division: https://www.anl.gov/es/article/analyzing-with-impact
- Chubbock, S. a. (2016). Comparative Analysis of Internal Combustion Engine and Fuel Cell Range Extender. SAE International Journal of Alternative Powertrains, 175-182, https://doi.org/10.4271/2016-01-1188.
- Elgowainy A, H. J. (2018). Current and Future United States Light-Duty Vehicle Pathways: Cradle-to-Grave Lifecycle Greenhouse Gas Emissions and Economic Assessment. *Environmental Science & Technology*, 52:2392–9. doi:10.1021/acs.est.7b06006.
- Engineers, S. o. (2014). Drive Quality Evaluation for Chassis Dynamometer Testing.
- Fuel Cell Technologies Office. (2012, updated 2016). *Multi-Year Research, Development, and Demonstration Plan.* Washington, DC: U.S. Departement of Energy. Retrieved from https://www.energy.gov/sites/prod/files/2017/05/f34/fcto_myrdd_fuel_cells.pdf
- Fuel Cell Technologies Office. (2015). DOE Technical Targets for Fuel Cell Systems and Stacks for Transportation Applications. Retrieved from U.S. Department of Energy: https://www.energy.gov/eere/fuelcells/doe-technical-targets-fuel-cell-systems-and-stacks-transportation-applications
- Hasegawa, T. I. (2016). Development of the Fuel Cell System in the Mirai FCV,. SAE 2016 World Congress and Exhibition. 2016-01-1185, p. 5. Detroit, MI: Society of Automotive Engineers. doi:https://doi.org/10.4271/2016-01-1185
- Heywood, J. (1988). *Internal Combustion Engine Fundamentals* (1st edition ed.). McGraw-Hill Education. doi:ISBN-10: 007028637X
- Kumar, A. a. (2018). Hydrogen Fuel Cell Technology for a Sustainable Future: A Review. *SAE Technical Paper*, 2018-01-1307, https://doi.org/10.4271/2018-01-1307.
- Kurtz, J. S. (2016). Fuel Cell Electric Vehicle. *2016 Annual Merit Review.* Washington DC: U.S. Department of Energy.
- Liu X., R. K.-B. (2019). Comparison of Well-to-Wheels Energy Use and Emissions of a Hydrogen Fuel Cell Electric Vehicle relative to a Conventional Gasoline-powered Internal Combustion Engine Vehicle. *Submitted to Int H2 Journal*.
- Lohse-Busch, H. (2011). APRF test. my own, 1. doi:asfdsadf
- Lohse-Busch, S. K. (2013, July). *Chassis Dynamometer Testing Reference Document*. Retrieved from Argonne National Laboratory: https://anl.app.box.com/s/5tlld40tjhhhtoj2tg0n4y3fkwdbs4m3
- Lynn K. Mytelka, . B. (2008). *Making Choices about Hydrogen: Transport Issues for Developing Countries.*Tokyo: United Nations University Press. doi:ISBN 978-9280811551
- National Institute of Standards and Technology. (2018). *NIST Chemistry WebBook*. Retrieved from webbook.nist.gov
- Salman, P. W.-O. (2017). Hydrogen-Powered Fuel Cell Range Extender Vehicle Long Driving Range with Zero-Emissions. *SAE Technical Paper*, 2017-01-1185, 2017, https://doi.org/10.4271/2017-01-1185.
- Society of Automotive Engineers. (2010, 03 12). SAE J1263 Road Load Measurement and Dynamometer Simulation Using Coastdown Techniques. Retrieved from www.sae.org/standards/content/j1263_201003/
- Society of Automotive Engineers. (2014, 01 24). SAE J2951 Drive Quality Evaluation for Chassis

 Dynamometer Testing. Retrieved from www.sae.org/standards/content/j2951 201401/
- Toyota. (2017, July 27). 2017 Toyota Mirai Product Information. Retrieved from Toyota USA Newsroom: https://toyotanews.pressroom.toyota.com/releases/2017+toyota+mirai+product.htm

- U.S. Environmental Protection Agency. (2019, March). *Data on Cars used for Testing Fuel Economy*. Retrieved from https://www.epa.gov/compliance-and-fuel-economy-data/data-cars-used-testing-fuel-economy
- Woosuk Sung, Y.-I. S.-H.-W. (2010). Recent Advances in the Development of Hyundai · Kia's Fuel Cell Electric Vehicles. *SAE International Journal of Engines*, 768-772. doi: https://doi.org/10.4271/2010-01-1089

Appendix A: Fuel and Energy Consumption Test Results for Comparison Vehicles in Section 4.6

Table A-1: Vehicle efficiency comparison across powertrain architectures

Powertrain	Fuel Cell				/ Electri	С	Hybrid Electric			Conventional			
Туре	Vehicle	<u> </u>		Vehicle			Vehicle			Vehicle			
Representative	2016 To	oyota		2017 Toyota Prius			2017 To	yota Priu	ıs	2014 Mazda 3			
Model	Mirai			Prime ir	n charge		Prime ir	n charge					
				depletir	ng mode		sustaini	sustaining mode					
Vehicle Testing	Equivaler	nt Test Weig	ght:			Equivalen	t Test Weig	ht:		Equivalent Test Weight:			
Characteristics	1928 kg (4250 lb)				1644 kg (3625 lb)			1559 kg (3438 lb)		
Characteristics	Target ro	ad load coe	fficients:			Target roa	ad load coefficients:			Target road load coefficients:			
	A = 143.8					A = 83.7 N				A = 102.9 N			
	B = 1.990				B = 3.850 N/(m/s)					B = 6.627 N/(m/s)			
	C = 0.407	2 N/(m/s) ²			$C = 0.2783 \text{ N/(m/s)}^2$				C = 0.2472 N/(m			ı/s) ²	
Test	-7°C	25°C	35°C	-7°C	25°C	35°C	-7°C	25°C	35°C	-7°C	25°C	35°C	
Temperature	(20°F)	(72°F)	(95°F)	(20°F)	(72°F)	(95°F)	(20°F)	(72°F)	(95°F)	(20°F)	(72°F)	(95°F)	
UDDS#1	581.1	226.3	321.2	224.2	106.8	143.6	361.9	242.1	349.8	872.7	662.3	722.1	
UDDS#2	347.9	217.3	279.1	206.8	104.3	128.5	380.6	245.5	324.4	643.0	595.7	675.3	
UDDS#3	258.7	209.8	288.2	0.0	103.5	128.6		237.5	293.8	638.2	595.7	696.5	
Highway#2	258.4	220.0	233.6	190.7 125.2 133.7			311.7	262.8	287.7	440.5	407.1	416.6	
US06#2	401.4	369.2	414.5	235.2	188.1	197.0	434.0	401.2	435.3	669.8	647.5	653.2	
		sumption] with 119		[AC Wh/	sumption 'km], which charging			sumption] with 0.7 08 J/g			sumption 1] with 0.7 02 J/g		

Table A-2: Fuel consumption and energy consumption across powertrain architectures

Powertrain	Fuel Cell			Battery Electric			Hybrid Electric			Conventional			
Туре	Vehicle	2		Vehicle	2		Vehicle			Vehicle			
Representative	2016 To	oyota			oyota Priu	ıs	2017 Toyota Prius			2014 Mazda 3			
Model	Mirai				n charge			n charge					
				depletii	ng mode			ing mode	!				
Vehicle Testing	Equivaler 1928 kg (nt Test Weig 4250 lb)	ght:			Equivalen 1644 kg (it Test Weig 3625 lb)	ght:		Equivaler 1559 kg (nt Test Weig 3438 lb)	ght:	
Characteristics	Target ro	ad load coe	efficients:				ad load coe	efficients:		Target ro	ad load coe	efficients:	
	A = 143.8 B = 1.990					A = 83.7 N				A = 102.9 B = 6.627			
		2 N/(m/s) ²				B = 3.850 C = 0.278	3 N/(m/s) ²				2 N/(m/s) ²		
Test	-7°C	25°C	35°C	-7°C	25°C	35°C	-7°C	25°C	35°C	-7°C	25°C	35°C	
Temperature	(20°F)	(72°F)	(95°F)	(20°F)	(72°F)	(95°F)	(20°F)	(72°F)	(95°F)	(20°F)	(72°F)	(95°F)	
•	Fu	el Econor	ny	Energ	y Consum	ption	Fu	iel Econor	ny	Fuel Economy			
		[mi/kg]		[.	AC Wh/m	i]		[mi/kg]		[mi/kg]			
UDDS#1 Cold start Phase 1	28.6	84.3		365	194		40.3	57.7		21.0	30.3		
UDDS#1 Cold start Phase 2	46.3	99.4		356	150		81.5	126.2		26.7	31.9		
UDDS#2 Hot	45.0	87.6		330	187		48.3	57.5		33.2	36.1		
start Phase 3	45.0	87.0		330	107		40.5	37.3		33.2	30.1		
UDDS#2 Hot	84.8	103.7		335	149		61.5	130.1		31.0	33.3		
start Phase 4													
Highway#2		94.1			202			75.0			50.6		
US06#2 City		38.9			359			29.8			20.3		
US06#2 Highway		64.1			294			58.6			38.0		
SC03#2			63.1			177			54.5			29.2	
City (5 cycle label)	5	7.4 mi/k	g	244 AC Wh/mi		56.9 mpg			25.6 mpg				
Highway (5 cycle label)	6	0.5 mi/k	κg	306 AC Wh/mi		/mi	54.4 mpg			35.4 mpg			
Combined													
Label Fuel	58.7 mi/kg			272	272 AC Wh/mi 55.7 mpg				g	2	29.3 mp	g	
Economy				·									
Combined													
Label Fuel	2.044 MJ/mi		0.8	0.817 MJ/mi 2.102 Mj/mi			mi	3.9	996 MJ/	mi			
Consumption													